Defects in plastically deformed semiconductors studied by positron annihilation: Silicon and germanium

R. Krause-Rehberg
Fachbereich Physik, Martin-Luther-Universität Halle-Wittenberg, Friedemann-Bach-Platz 6, D(O)-4020 Halle/Saale, Federal Republic of Germany

M. Brohl
Abteilung Metallphysik, II. Physikalisches Institut, Universität Köln, Zülpicher Strasse 77, D-5000 Köln, Federal Republic of Germany

H. S. Leipner, Th. Drost, A. Polity, and U. Beyer
Fachbereich Physik, Martin-Luther-Universität Halle-Wittenberg, Friedemann-Bach-Platz 6, D(O)-4020 Halle/Saale, Federal Republic of Germany

H. Alexander
Abteilung Metallphysik, II. Physikalisches Institut, Universität Köln, Zülpicher Strasse 77, D-5000 Köln, Federal Republic of Germany
(Received 26 October 1992)

This paper is concerned with positron-annihilation studies in floating-zone silicon, which has been plastically deformed under high-stress and low-temperature conditions (HSLT). Positron lifetime spectra were decomposed into three components by means of the trapping model. Two defect-related lifetimes were found to be constant ($\tau_2=300$ ps and $\tau_3=590$ ps); they are constant during annealing. They are attributed to positron capture and annihilation by dislocation states (τ_2) and microvoids (τ_3). The microvoids (vacancy clusters) consist of at least ten vacancies. According to the model of diffusion-limited positron trapping, an upper limit of the microvoid concentrations is estimated. A pronounced increase of the microvoid-related trapping rate was observed after 600 °C annealing of samples macroscopically deformed in the HSLT step. The positron capture to dislocations is also described as diffusion limited and the dislocation densities obtained agree satisfactorily with densities measured by transmission electron microscopy. Nonconservative dislocation motion and relaxation (jog dragging) during annealing is proposed as an efficient vacancy-generation process. Similar clustering effects were observed for HSLT-deformed high-purity germanium at appropriately lower temperatures. The characteristic defect-related positron lifetimes in Ge are determined to be $\tau_2=325$ ps and $\tau_3=520$ ps for dislocations and microvoids, respectively.

I. INTRODUCTION

The plastic deformation of floating-zone (FZ) silicon leads to the formation of a variety of point-defect-related centers, which are active, e.g., in deep-level transient spectroscopy[1-3] (DLTS) or electron paramagnetic resonance[4-6] (EPR). Based on structural models, the unambiguous identification has been possible only in a few cases, as for well-known irradiation defects (e.g., for the EPR centers $K3$, $K4$, and $K5$, see Ref. 4). This is due to the complex signal superposition in EPR and DLTS. Furthermore, the competition of defect production and annealing during plastic deformation at the deformation temperature $T_{\rm def}\approx 650$ °C is not well understood. There is evidence from EPR experiments that vacancy clusters possibly bound to impurities are the dominant paramagnetic centers[4,6] but sufficient structural information is still lacking.

The lowering of deformation temperatures down to 400 °C demands high stresses ($\tau=200$ MPa) and a higher skill level. On the other hand, it permits the identification of part of the deformation-induced EPR spectrum as $P1$.[7] According to Lee and Corbett,[8] this defect is associated with a pentavacancy cluster, which is typically a secondary product of neutron irradiation. It is supposed that vacancies emitted by dislocations moving under high applied glide forces cluster at 400 °C. Thus, the understanding of defect morphologies seems to be easier under high-stress and low-temperature (HSLT) deformation.

Positron annihilation (PA) spectroscopy is primarily sensitive to open volume defects, such as vacancies, microvoids (vacancy clusters), and dislocations in the bulk of crystals.[9,10] Therefore, the PA technique is a suitable tool for the investigation of vacancy clusters induced by plastic deformation. The positron lifetime gives information about local electron densities around defects and can be correlated under certain conditions to the size of the open volume, i.e., the number of vacancies involved.[9,10] The capture rate of a given defect depends on the defect concentration.

Moreover, the sensitivity of the positron trapping is a function of the charge of the trapping center. In the case of negatively charged defects, the positron trapping rate

shows a strong increase at low temperatures ($T < 100$ K),[11–13] while neutral defects cause no comparable temperature-dependent trapping effect. Finally, positrons are not sensitive to positively charged defects due to their repelling force.

In the following, PA studies of HSLT-deformed silicon in the as-deformed state and after annealing up to 850 °C are presented. The location of the Fermi level in the band gap could be controlled by a suitable choice of dopant and its concentration. Furthermore, first results are included for PA in high-purity germanium, where a similar HSLT deformation cycle was applied. Corresponding experiments on defects in plastically deformed GaAs will be presented elsewhere.

II. EXPERIMENT

A. Plastic deformation

The Si samples used in this study were FZ single crystals (grown by Wacker Chemitronics) uniaxially deformed along the [213] compression axis. In order to provide a sufficient dislocation density for plastic deformation at a low temperature, the first step was a predeformation at the temperature $T_{def}=800$ °C up to a strain of $\varepsilon=0.8-1.6$ % with the resolved shear stress in the primary glide system $\tau=12$ MPa. Typical dislocation densities were $N_{dis}\approx(5-10)\times10^7$ cm^{-2} in similarly deformed samples. A subsequent annealing (800 °C, time $t\geq10$ min) and a slow cooling ramp down to 400 °C ($t\geq2$ h) served to reduce the density of residual DLTS- and EPR-active levels (typically $N_{EPR,DLTS}\approx10^{14}$ cm^{-3}).[2] For the main deformation at 400 °C two different methods were chosen. Sample Si-*A* underwent a short HSLT deformation with $\tau=250$ MPa ($t=30$ min). By this method, dislocation loops were extended to form regular hexagonal configurations of widely dissociated 60° and screw dislocation segments, mainly arranged in the primary glide plane.[14] No dislocation glide could be measured macroscopically (additional strain $\Delta\varepsilon<0.05\%$). The dislocation density increased to $N_{dis}\approx4\times10^8$ cm^{-2}. The DLTS defect density N_{DLTS} was very low (about 2×10^{14} cm^{-3}). The crystals Si-*B*, *C*, *D*, and *E* were deformed under HSLT conditions ($\tau=200$ MPa) up to $\Delta\varepsilon=0.6-1.4$ % for $t=36-48$ h. N_{dis} was determined to be $(3-6)\times10^9$ cm^{-2} by transmission electron microscopy (TEM) in the samples Si-*B* and *C*. N_{DLTS} was about 2×10^{15} cm^{-3}. Finally, all crystals were cooled down to room temperature under the applied force to freeze in the defect configurations. Table I summarizes the doping and deformation conditions for silicon samples.

As a first experimental approach for germanium, the same method of discriminating between deformation structures of high and low dislocation glide at low temperatures was chosen, leading to high and low point-defect densities. Two high-purity crystals (intrinsic, carrier concentration $\approx5\times10^{12}$ cm^{-3}), labeled Ge-*A* and Ge-*B*, were predeformed at 550 °C ($\tau=12$ MPa; Ge-*A*: $\varepsilon=2\%$; Ge-*B*: $\varepsilon=1\%$) and slowly cooled down to 220 °C and then deformed with $\tau=250$ MPa for 30 min ($\Delta\varepsilon<0.05\%$; Ge-*A*) and 20 h ($\Delta\varepsilon=0.9\%$; Ge-*B*), respectively. The dislocation density in as-deformed Ge was determined by TEM to be 2×10^9 cm^{-2} (Ge-*B*).

B. Positron annihilation

Positron lifetime spectroscopy was used for this study. Positrons were supplied by a weak radioactive (6×10^5 Bq) ^{22}NaCl source. The source (active size 1×1 mm^2) was covered with two Al foils of 1.5-μm thickness and placed between a pair of samples. The samples, which were prepared by cutting and standard polishing techniques, were two adjacent slices (600-μm thick) near the middle of the deformed specimens. The lifetime spectra were recorded in samples in the as-deformed state and after annealing. Undeformed crystals were also measured for reference. The isochronal annealing was carried out in an Ar atmosphere in 25 K steps for 30 min.

The positron lifetime spectrum was monitored by measuring the time difference between the positron birth in the source indicated by a 1.28-MeV γ quantum, and the annihilation γ rays of 0.51 MeV, using a conventional fast-slow coincidence system (time resolution 230 ps). About 2×10^6 counts were collected during 2 h. The lifetime spectrum was analyzed with the trapping model

TABLE I. Doping and deformation conditions of Si crystals used in this study. The integral number of DLTS-active centers and effective free-carrier concentrations after deformation are also included.

Sample	Dopant	Doping concentration (cm^{-3})	Predeformation $T_{def}=800$ °C/$\tau=12$ MPa ε (%)	Main deformation T_{def} (°C)/τ (MPa) $\Delta\varepsilon$ (%)	N_{DLTS} (cm^{-3})	Free-carrier concentration at 20 °C (cm^{-3})
Si-*A*	P	4.4×10^{15}	1.6	420/250 <0.05	2×10^{14}	$\approx4\times10^{15}$
Si-*B*	P	4.4×10^{15}	0.8	390/200 0.6	1×10^{15}	$\approx3\times10^{15}$
Si-*C*	P	2×10^{13}	0.9	390/200 1.4	2×10^{15}[a]	$<1\times10^{13}$
Si-*D*	P	5×10^{16}	0.9	390/200 0.6		$\approx5\times10^{16}$
Si-*E*	B	5×10^{16}	0.9	390/200 0.6		$\approx5\times10^{16}$

[a]Estimation according to C. Kisielowski-Kemmerich and H. Alexander, in *Defects in Crystals,* edited by E. Mizera (World Scientific, Singapore, 1988), p. 290.

after subtracting the source and background contribution.

C. Analysis of lifetime spectra

The positron lifetime spectrum is considered as a sum of exponential decay terms, where I_i and τ_i are the intensities and the lifetimes of the component i.[15] The positron lifetime spectrum consists of two components in case of one dominant defect type. The second component is constant and related to the electron density of the defect d, and its intensity reflects the defect concentration. In case of transition-limited trapping[16] the trapping rate κ_d is proportional to the defect concentration N_d,

$$\kappa_d = \mu_d N_d \ . \tag{1}$$

The so-called specific trapping rate μ_d is a constant for a given defect type at a certain temperature. For extended traps such as voids the positron trapping is no longer transition limited but diffusion limited. The trapping rate is now proportional to the product of the defect density N_d and the radius r of the defect, which is assumed to be spherical. The trapping rate is calculated by

$$\kappa_d = 4\pi D_+ r N_d \ , \tag{2}$$

where D_+ is the positron diffusion constant.[16]

In the simple trapping model (one-defect type, no interaction of individual defects, no escape of trapped positrons),[16] the lifetimes τ_1, τ_2 and intensities I_1, I_2 are given by

$$\tau_1 = \frac{1}{\frac{1}{\tau_b}+\kappa_d} \ ,$$

$$\tau_2 = \tau_d \ , \quad I_1 = 1 - I_2 \ , \tag{3}$$

$$I_2 = \frac{\kappa_d}{\frac{1}{\tau_b}+\kappa_d-\frac{1}{\tau_d}} \ ,$$

where τ_b and τ_d are the positron lifetimes in the bulk and at the defect. The trapping rate κ_d can be calculated from the decomposition of the lifetime spectra according to Eq. (3). It is possible to check whether the choice of the two-component model (one dominant defect) is reasonable. If the supposition of the one-defect trapping model is valid, the lifetime $\tau_{1,\mathrm{model}}$ calculated with Eq. (3) should coincide with the measured lifetime $\tau_{1,\mathrm{exp}}$.

In the case of two dominant positron traps d_1 and d_2 (i.e., three lifetime components) which are independent of each other (e.g., dislocations and microvoids), the lifetime components τ_i and their intensities I_i ($i=1,2,3$) can be derived in the following way (capture model 1):

$$\tau_1 = \frac{1}{\frac{1}{\tau_b}+\kappa_{d_1}+\kappa_{d_2}} \ , \quad \tau_2 = \tau_{d_1} \ , \quad \tau_3 = \tau_{d_2} \ ,$$

$$I_1 = 1-(I_2+I_3) \ ,$$

$$I_2 = \frac{\kappa_{d_1}}{\frac{1}{\tau_b}+\kappa_{d_1}+\kappa_{d_2}-\frac{1}{\tau_{d_1}}} \ , \quad I_3 = \frac{\kappa_{d_2}}{\frac{1}{\tau_b}+\kappa_{d_1}+\kappa_{d_2}-\frac{1}{\tau_{d_2}}} \ . \tag{4}$$

Capture model 2 describes the situation that the defects are not independent of each other.[17] A possible example is that microvoids (defect d_2) are located on dislocation lines (defect d_1). The positrons are first trapped by dislocations and move along the dislocation line until they are trapped by the microvoids. The components of the lifetime spectra are then determined by Eq. (5) as

$$\tau_1 = \frac{1}{\frac{1}{\tau_b}+\kappa_{d_1}} \ , \quad \tau_2 = \frac{1}{\frac{1}{\tau_{d_1}}+\kappa_{d_2}} \ , \quad \tau_3 = \tau_{d_2} \ ,$$

$$I_1 = 1-(I_2+I_3) \ ,$$

$$I_2 = \frac{\kappa_{d_1}\left[\frac{1}{\tau_{d_1}}-\frac{1}{\tau_{d_2}}\right]}{\left[\frac{1}{\tau_{d_2}}-\frac{1}{\tau_{d_1}}-\kappa_{d_2}\right]\left[\frac{1}{\tau_{d_1}}+\kappa_{d_2}-\frac{1}{\tau_b}-\kappa_{d_1}\right]} \ , \tag{5}$$

$$I_3 = \frac{\kappa_{d_1}\kappa_{d_2}}{\left[\frac{1}{\tau_{d_2}}-\frac{1}{\tau_b}-\kappa_{d_1}\right]\left[\frac{1}{\tau_{d_2}}-\frac{1}{\tau_{d_1}}-\kappa_{d_2}\right]} \ .$$

The second lifetime τ_2 is no longer constant, but dependent on the trapping rate κ_{d2}, i.e., dependent on the density of microvoids. (This is also valid in the case where thermal detrapping from the dislocation line is taken into account.[17]) Furthermore, this lifetime component is expected to become rather small if the trapping rate κ_{d2} is remarkably different from zero.

III. RESULTS

The average positron lifetime $\bar{\tau}$ after isochronal annealing (30 min in 25-K steps) is shown in Fig. 1. In the as-deformed samples Si-*A* and Ge-*A*, a small increase in comparison with the average lifetime in undeformed materials (Si: $\tau_b = 218$ ps; Ge: $\tau_b = 230$ ps) was obtained, $\bar{\tau} = 220$ and 234 ps, respectively. In contrast, the specimens Si-*B*, Si-*C*, and Ge-*B* exhibit a remarkable increase of $\bar{\tau} = 270$ ps (Si) and 340 ps (Ge) by deformation. A pronounced maximum (320 ps) appeared at 600 °C in samples Si-*B* and *C*. The differences between both samples were small. A similar maximum was found at the same reduced temperature of $0.5T_M$ (T_M is the melting temperature) in Ge-*B*. In both cases, the average lifetime reached the level of the weakly deformed samples after annealing at $0.7T_M$.

In order to obtain detailed information about the defects involved in positron trapping the decomposition of the spectra is necessary. Both two- and three-component fits were applied to the data. The results of the fits are shown in Figs. 2–4. In general, the three-component fit provided better results: the variance of fit was in all cases

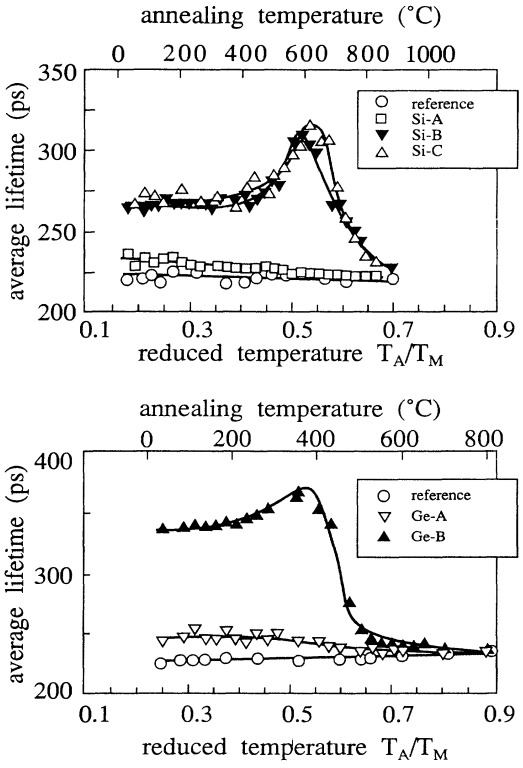

FIG. 1. Average positron lifetime $\bar{\tau}$ of plastically deformed Si and Ge single crystals vs the annealing temperature T_A reduced to the melting temperature T_M.

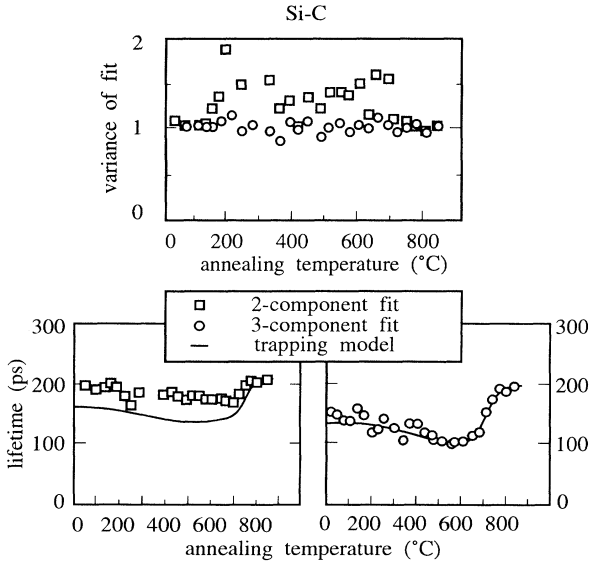

FIG. 2. Variance of fit and lifetimes in terms of the trapping model for a two- and three-component fit in the sample Si-*C*. The diagrams below show the measured lifetime $\tau_{1,\mathrm{exp}}$ together with the calculated $\tau_{1,\mathrm{model}}$ (solid line) for both approaches.

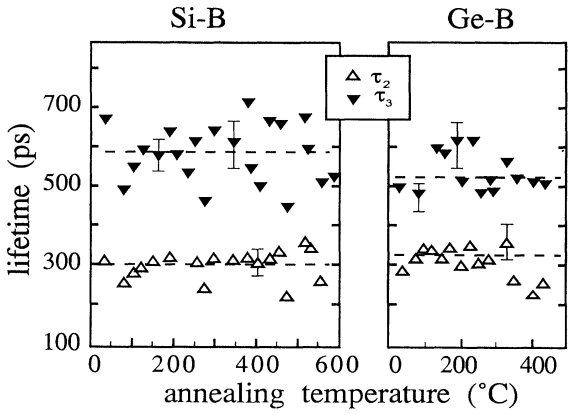

FIG. 3. Second and third lifetime component τ_2 and τ_3 as a function of the annealing temperature T_A in Si-*B* and Ge-*B*. The dashed lines represent the average values.

close to 1. Furthermore, the calculated lifetime $\tau_{1,\mathrm{model}}$ differed systematically from the experimental value in the case of two types of defects trapping positrons. The results of sample Si-*C* are presented as a typical example in Fig. 2. Similar results were obtained in samples Si-*B* and Si-*D*. In sample Si-*A*, being only weakly deformed and causing a small trapping effect, a two-component fit was also suitable.

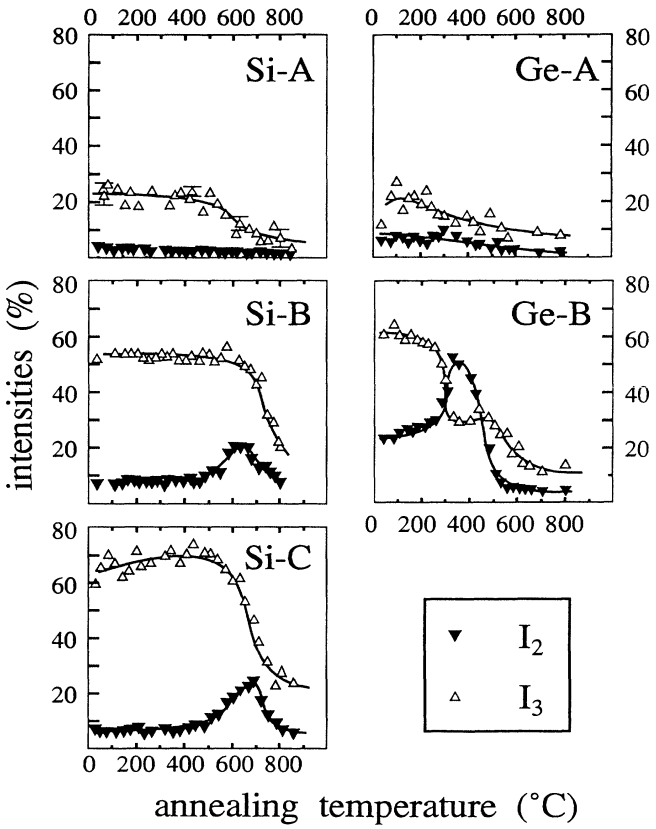

FIG. 4. Intensities I_2 and I_3 vs annealing temperature for deformed Si and Ge. Intensity I_1 is not given, since $I_1+I_2+I_3=1$.

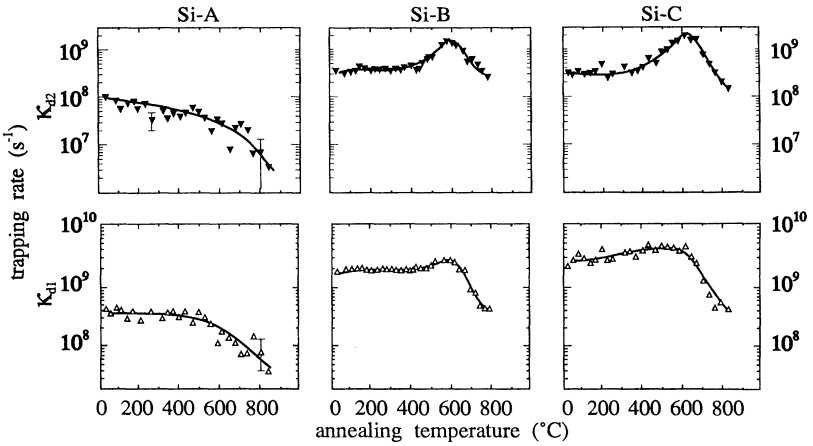

FIG. 5. Positron trapping rates κ_{d1} (dislocations) and κ_{d2} (microvoids) vs annealing temperature T_A in deformed Si.

The results are very similar for germanium. Again, the two-component fit did not describe the measured spectra properly. Thus, a three-component fit was applied to all spectra. The second and third lifetime components τ_2 and τ_3 are shown in Fig. 3 as a function of the annealing temperature for the samples Si-*B* and Ge-*B*. For Si, the scatter of τ_3 is rather high as usual for a free three-component fit, but no clear tendency is visible. The average values are $\tau_2=300$ ps and $\tau_3=590$ ps. For Ge, the average values are $\tau_2=325$ ps and $\tau_3=520$ ps. The positron trapping decreases drastically above 500 °C. Thus, no direct three-component decomposition of the spectra was possible there. In order to compare the results obtained below 500 °C with those above 500 °C, the lifetimes have been fixed to their values obtained at lower annealing temperatures (Fig. 3) in the whole temperature range.

Figure 4 shows the intensities of the three-component decomposition of the lifetime spectra. The intensities were used to calculate the trapping rates κ_{d1} and κ_{d2} of the corresponding defect types d_1 and d_2 (Figs. 5 and 6) with Eq. (4). The results of sample Si-*D* are similar to those of Si-*B* and are not shown in the figures. A pronounced maximum of the trapping rate κ_{d2} occurred for both strongly deformed materials around $0.5T_M$, while the trapping rate κ_{d1} in Ge-*B* stays constant up to the onset of the annealing stage at 340 °C ($0.5T_M$). A small increase of κ_{d1} appears for Si-*B*. The increase is rather weak (factor of 1.5) and might be an artificial effect of the three-component decomposition due to the incomplete separation of the lifetime components.

The temperature dependence of the positron trapping was studied between 50 and 600 K. As an example, the results of the three-component decomposition of sample Si-*B* is shown in Fig. 7. Again, two defect-related life-

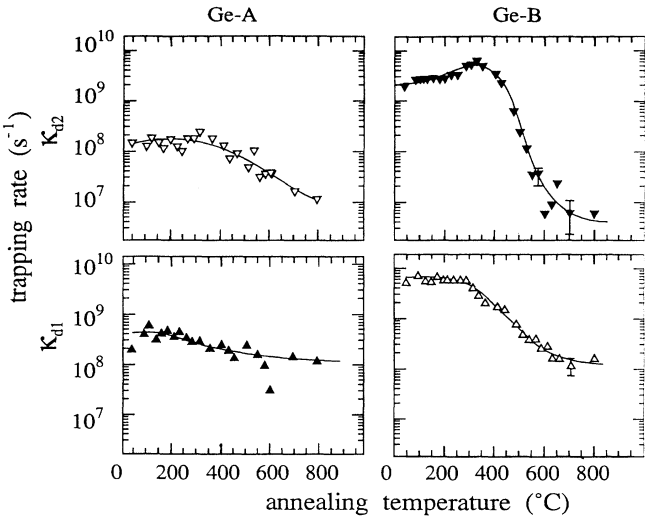

FIG. 6. Trapping rates κ_{d1} (dislocations) and κ_{d2} (microvoids) vs annealing temperature in deformed Ge.

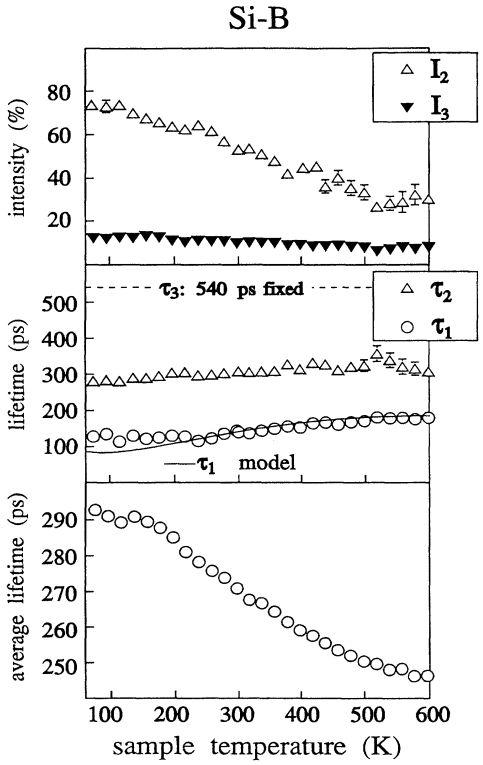

FIG. 7. Results of the three-component decomposition of temperature-dependent lifetime measurements in Si-*B*. The solid line corresponds to the first lifetime τ_1, calculated according to the capture model 1 [Eq. (4)].

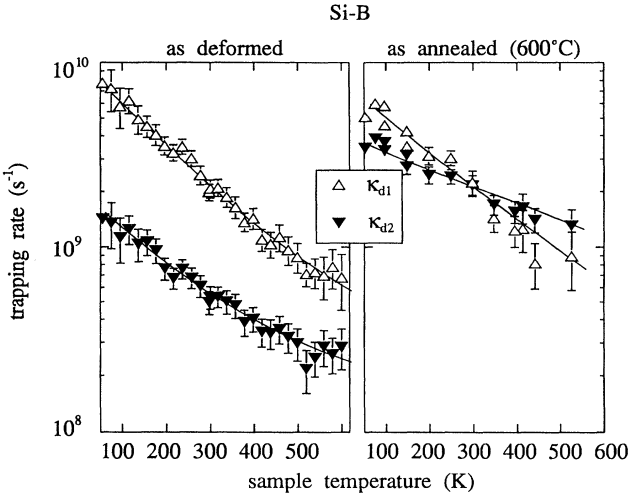

FIG. 8. The temperature dependence of the positron trapping rates κ_{d1} and κ_{d2} in the sample Si-*B* in the as-deformed state (left-hand side) and after annealing at 600 °C (30 min).

times could be separated, $\tau_2=300$ ps and $\tau_3=540$ ps. These values correspond to the lifetime values obtained for the annealing measurements within the error limits and the uncertainties of the decomposition procedure. The whole temperature behavior was completely reversible and the longest lifetime τ_3 did not show any temperature dependence. In order to reduce the scatter of the intensities and the trapping rates, the lifetime τ_3 was fixed to its average value (dashed line in Fig. 7). The calculated trapping rates are shown versus the sample temperature in Fig. 8. The results are compared with the temperature dependence of the positron trapping after annealing at 600 °C (30 min) on the right-hand side of Fig. 8.

IV. DISCUSSION

A. Trapping rates and defect densities

1. n-type material

The two defect-related lifetimes observed (Si: $\tau_2=300$ ps and $\tau_3=590$ ps; Ge: $\tau_2=325$ ps and $\tau_3=525$ ps) are attributed in this paper to dislocations (defect d_1) and microvoids (defect d_2). The corresponding arguments for this attribution are given later in this section.

Since the positron bulk lifetime in Si is $\tau_b=218$ ps, all deformed samples show a pronounced positron trapping by defects. In order to study the defects involved, the decomposition of the lifetime spectra into their components is necessary. As described in Sec. III, only three-component fits provided reliable results. The intensities obtained (Fig. 4) were used to calculate the positron trapping rates in terms of the capture model 1 of Eq. (4) supposing two independent traps d_1 and d_2. In order to reduce the scatter of the intensities, the lifetimes were fixed to their average values as given above. It is possible to do this within the framework of capture model 1, because the lifetimes τ_2 and τ_3 have to be constant according to Eq. (4). They are independent of the defect concentration. In fact, no systematic dependence was observed (Fig. 3).

Regarding the discussion in Sec. II C, it is concluded that the capture model 2 (i.e., defects d_1 and d_2 are not independent) cannot be valid. A simple example shows that the second lifetime component should be very small and dependent on the concentration of microvoids: Assuming a trapping rate κ_{d2} that yields a remarkable trapping to the microvoids, e.g., $\kappa_{d2}=0.5(1/\tau_b)$, a lifetime $\tau_2=146$ ps should be found in Si [according to Eq. (5)]. This is even much smaller than the bulk lifetime $\tau_b=218$ ps. Furthermore, a lifetime $\tau_1=1/(\kappa_{d1}+1/\tau_b)\leq 218$ ps, depending on the actual value of κ_{d1}, would be expected. Even if $\tau_2=146$ ps is compared with the experimentally determined shortest lifetime (Fig. 2), $\tau_2\leq 218$ ps does not fit the experimental findings (300 ps). Thus, it is concluded that the corresponding capture model 2 (positrons are *first* trapped by dislocations and then located at microvoids at the dislocation line) does not describe the positron trapping in the material. Consequently, the capture model 1 (positrons are trapped by two independent types of defects) was applied to calculate the positron trapping rates [Eq. (4)].

However, the spatial association between dislocations and microvoids cannot be completely excluded by the argument given above. It can only be excluded that positrons find the microvoids by migrating along the one-dimensional trapping potential of the dislocation line. Microvoids localized at the dislocation line might also be found by positrons directly on their diffusion way, without being trapped by the dislocation before. This seems to be likely, because the specific positron trapping rate for microvoids is generally rather high. Thus, the two different positron traps are found independently from each other and the suppositions of capture model 1 would also be fulfilled in this case.

Such long lifetimes as obtained (Si: $\tau_3=590$ ps; Ge: 520 ps) can only be attributed to microvoids (defect d_2). A lifetime of 500 ps has been attributed to the largest possible lifetime in defects in metals and semiconductors as a result of semiempirical estimations of the lower limit of the electron density.[18] Moreover, the dependence of the positron lifetime on the size of vacancy clusters in Si was calculated by Puska and Corbel.[19] The lifetime increases with the number of vacancies n and tends to saturate at $\tau\approx 500$ ps. According to the results of Puska and Corbel,[19] one has to conclude that the clusters observed in this study are rather large and the size is $n\geq 10$. Positron trapping to such large clusters is usually believed to be diffusion limited[16] and has to be handled with Eq. (2). Since the lifetime is already saturated, a further growth of the microvoids would not lead to a further remarkable increase of τ_3. Similar to our results, Dannefaer, Mascher, and Kerr[20] and Saarinen *et al.*[21] found a long-lifetime component in GaAs of about 500 ps, which they attributed to voids. It should be added that the formation of positronium cannot be excluded in view of the extremely large τ_3.[22]

The lifetime τ_2 (Si: 300 ps; Ge: 325 ps) is attributed to positron trapping at dislocations (defect d_1). The dislocation density $N_{\rm dis}$ was determined by TEM (Si-A: 4×10^8 cm^{-2}; Si-B: 2.5×10^9 cm^{-2}; Ge-B: 2×10^9 cm^{-2}). Thus,

the dislocation density is within the expected sensitivity range of the positron method. According to Brandt and Paulin,[23] the positron trapping to dislocation is diffusion limited and Eq. (2) has to be modified due to the cylindrical shape of the trap,

$$\kappa = \frac{4\pi D_+ N_{\text{dis}}}{\ln(\pi N_{\text{dis}} r^2)^{-1}} \ . \tag{6}$$

The trapping rate does not depend very much on the radius of the cylinder r. From the trapping rates experimentally obtained, the dislocation density was determined with two extreme arbitrarily chosen values of the cylinder radius $r_{\min}=0.1$ nm and $r_{\max}=5$ nm (Table II). The dislocation density determined by the positron trapping rate with Eq. (6) seems to be smaller than the density obtained by TEM. On the other hand, the experimental error for the determination of the dislocation density is of the order of 50%. Furthermore, positron annihilation provides integral defect information over the source dimension (1×1 mm^2). Therefore, the results cannot directly be compared to the results of electron microscopy. The fact that the dislocations are not completely homogeneously distributed (Fig. 9) may decrease the positron trapping rate. In conclusion, the agreement between the results of both methods may still be satisfying.

The trapping to dislocations has been described earlier as a transition-limited process [Eq. (1)], see, e.g., Dannefaer *et al.*[24] In the framework of such a model, the specific positron trapping rate of trapping to dislocations can be calculated for Si as $\mu_{\text{dis}}=(0.7\pm0.3)$ cm^{2}s^{-1} [Ge: $\mu_{\text{dis}}=(4\pm1)$ cm^{2}s^{-1}] following Eq. (1). However, this transition-limited process should lead to a temperature-independent trapping rate.

On the other hand, the trapping rate according to Eq. (6) (diffusion-limited trapping) is almost proportional to the dislocation density for a given radius r. Only a weak deviation is caused by the nominator in Eq. (6), e.g., a change in the dislocation density between 10^7–10^9 cm^{-2} changes the nominator by a factor of 0.8 or 0.6 ($r=0.1$ or 5 nm). Numerically, the description of the trapping to dislocations by Eq. (1) (transition-limited process) and by Eq. (6) (diffusion-limited trapping) leads to similar results.

TABLE II. Comparison of calculated [Eq. (6)] and dislocation densities measured by TEM. The calculated density range corresponds to the minimum and maximum values of the radius r (0.1 and 5 nm), respectively.

Sample		N_{dis} (cm^{-2}) calculated $r=5$ nm	$r=0.1$ nm	N_{dis} (cm^{-2}) measured
Si-*A*	as-deformed	1.4×10^8	2.6×10^8	4×10^8
	annealed 850 °C	1.8×10^7	2.9×10^7	1×10^8
Si-*B*	as-deformed	6.1×10^8	1.2×10^9	2.5×10^9
	annealed 850 °	1.4×10^8	2.6×10^8	
Si-*C*	as-deformed	8.7×10^8	1.7×10^9	4.5×10^9
	annealed 850 °C	1.4×10^8	2.6×10^8	4×10^8
Ge-*A*	as-deformed	1.4×10^8	2.6×10^8	
	annealed 800 °C	4.1×10^7	7.0×10^7	
Ge-*B*	as-deformed	1.8×10^9	3.8×10^9	2×10^9
	annealed 800 °C	5.6×10^7	1.0×10^8	

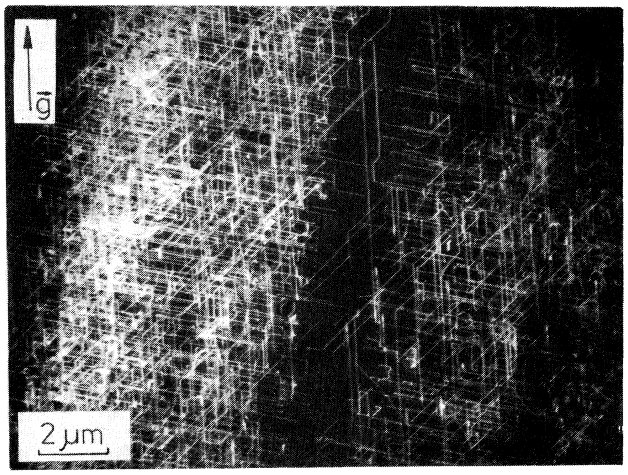

FIG. 9. Distribution of dislocations in Si-*C*. TEM weak beam (g-3g condition) taken at 1000 kV, (213) foil orientation, diffraction vector $\mathbf{g}=\bar{2}20$.

It should be noted that positrons may show different trapping behavior to different dislocation types (e.g., screws and 60° dislocations). Thus, the discussion of the relation between total dislocation density N_{dis} and positron trapping rate κ [Eq. (6)] is a simplified approach. It is likely that the positron interaction with screw dislocations is different, due to vacancylike defects observed by EPR in the dislocation core.[6] The difference in the calculated and measured dislocation densities N_{dis} by a factor of 1.5–3.5 for various Si samples (Table II) is then not merely due to uncertainties of the measurement as discussed above, but also to the fact that positrons may be differently sensitive to different dislocation types.

The measured dependence of the trapping rates on the sample temperature shows a distinct negative slope as expected for diffusion-limited trapping (see further discussion below). Thus, the model of diffusion-limited trapping to dislocations is favored.

The lifetime of $\tau_2=300$ ps could also be understood by the presence of divacancies (expected lifetime 306 ps, Ref. 19). On the other hand, it was found that divacancies in electron-irradiated Si anneal at about $T_A=200$ °C.[25] However, the measured annealing behavior (see discussion below) of the corresponding trapping rate does not show any changes in this temperature range.

Figures 5 and 6 show the calculated trapping rates. The dislocation trapping rate in Si remained unchanged up to the annealing temperature $T_A=600$ °C (Ge: 300 °C) and was then reduced by one order of magnitude within about 350 K (sample Si-*A*) and 200 K (sample Si-*B* and Si-*C*; Ge: 250 K). The trapping rate κ_{d1} did not vanish even at the highest applied annealing temperature $T_A=850$ °C. The calculated dislocation density after annealing (Si-*A*, Table II) is slightly above the sensitivity limit of the PA method and corresponds—with respect to the higher error in this region—to the density found by TEM, $N_{\text{dis}}=1\times10^8$ cm^{-2}.

An estimation of the upper limit of the density of mi-

crovoids N_{void} can be given. Assuming spherical microvoids, the trapping rate is obtained [Eq. (2)]. According to the discussion of the large positron lifetime in the microvoids, the size $n \geq 10$ is expected. This value corresponds to the effective microvoid radius $r \geq 0.4$ nm. The radius can be calculated by

$$r = \frac{a}{4}\sqrt{2}\sqrt[3]{n} , \quad (7)$$

supposing the model of close-packed hard spheres (a is the lattice constant). Thus, the upper limit of N_{void} is estimated with $D_+ = 2\ cm^2 s^{-1}$ for Si and Ge (Refs. 26 and 27) and is shown in Table III. For the higher deformed Si and Ge samples (B and C) a pronounced maximum of the trapping rate κ_{d2} is observed. Several possibilities to explain the maximum will be discussed in the following.

(1) The microvoids remain the same size and their density increases. This assumption seems to be reasonable considering the calculation of the stability of differently sized microvoids in Si.[28] According to Chadi and Chang,[28] microvoids of 6 or 10 vacancies are particularly stable. Since the trapping rate is proportional to the density of voids N_{void}, the increase of κ_{d2} by a factor of 6 may be understood by the increase of the density of microvoids by the same factor.

(2) The density of microvoids is constant and their size increases with further annealing. The increase of the trapping rate obtained (factor 6) can then be explained by the enlargement of the radius by a factor of 6. For this purpose, the number of vacancies to be built in has to increase by a factor of about 200 during annealing at 650 °C. This seems to be unlikely.

(3) Assuming the existence of a size distribution of the microvoids, the larger microvoids may grow more rapidly than the smaller ones, similar to Ostwald ripening. However, this process will always lead to a reduction of the trapping rate, $\kappa = 4\pi D_+ r N_{void}$. The radius of the enlarging microvoids increases by not more than a factor of $f^{1/3}$ by decreasing the density of microvoids N_{void} by a factor f. Thus, an overall decrease is obtained.

(4) Since the trapping to extended microvoids is diffusion limited, a dependence of the diffusion constant D_+ on the annealing has to be considered. The positron diffusion in Si and Ge is determined by scattering processes at phonons (acoustical and optical) and at scattering centers such as impurities or lattice defects.[26] Only the latter ones are possible candidates for annealing. It cannot be excluded that defects created during deformation limit the positron diffusion. In that case, their annealing would increase the positron diffusion constant D_+ and thus the trapping rate [Eq. (2)].

The dependence of scattering by phonons and defects on sample temperature is distinctly different.[26] For the scattering at phonons a negative temperature dependence is expected ($D_+ \sim T^{-1/2}$ and $T^{-3/2}$ for acoustical and optical phonons, respectively). Scattering at impurities or lattice defects will lead to a positive temperature dependence ($D_+ \sim T^{1/2}$ or $T^{3/2}$ for neutral or charged centers). In order to check the dominating scattering mechanism the temperature dependence of both positron trapping rates κ_{d1} and κ_{d2} was measured in the as-deformed state and after annealing at 600 °C of sample Si-B.

TABLE III. Upper limits of the microvoid densities calculated by Eq. (2) and a minimum size of $n = 10$.

Sample		N_{void} (cm^{-3})
Si-A	as-deformed	9.6×10^{13}
	annealed 850 °C	2.9×10^{12}
Si-B	as-deformed	3.3×10^{14}
	annealed 600 °C	1.4×10^{15}
	annealed 850 °C	1.9×10^{14}
Si-C	as-deformed	3.1×10^{14}
	anealed 600 °C	1.9×10^{15}
	annealed 850 °C	1.4×10^{14}
Ge-A	as-deformed	1.4×10^{14}
	annealed 800 °C	1.4×10^{13}
Ge-B	as-deformed	1.8×10^{15}
	annealed 350 °C	5.4×10^{15}
	annealed 800 °C	3.7×10^{12}

Figure 7 shows the results of the three-component decomposition in the as-deformed state. The longest lifetime was found to be temperature independent. It was fixed to its average value, $\tau_3 = 540$ ps. In order to check the validity of the chosen model, the values τ_1 were additionally calculated with Eq. (4) (solid line) and were compared to the experimental values. The agreement is satisfying. The deviation in the low-temperature range is due to the fact that values of $\tau_1 < 100$ ps usually cannot be resolved due to the limited time resolution. The measured temperature dependence of lifetimes and intensities after annealing at 600 °C is not shown. The positron trapping rates were calculated for the as-deformed and annealed state with Eq. (4) and are shown in Fig. 8.

In the as-deformed state (left diagram) both trapping rates follow a strong negative temperature dependence. This indicates that the positron diffusion at 300 K (being the temperature where the positron measurements of the annealing experiments were performed) is not governed by scattering at impurities or defects.

On the other hand, the temperature dependence of the trapping rate does not follow the $T^{-1/2}$ dependence expected for the scattering at acoustical phonons. According to Soininen *et al.*,[26] the scattering at acoustical phonons should limit the diffusion in the investigated temperature range in case no scattering at defects occurs. Both obtained trapping rates are approximately proportional to T^{-1}. Different temperature-dependent mechanisms may influence the temperature dependence of the positron trapping rate and will not be discussed in detail (e.g., increasing reflection at the potential responsible for positron trapping with decreasing temperature, temperature-dependent positron trapping due to band-bending effects near charged defects).

In the right-hand diagram of Fig. 8 the temperature dependence of the positron trapping after 600 °C annealing is plotted. The pronounced increase of the trapping rate κ_{d2} is visible. The slope of the temperature dependence is still negative and is not much changed. This is a further proof that the increase of the trapping rate κ_{d2} during annealing is not due to the increased positron

diffusion after possible annealing of deformation-induced defects acting as scattering centers.

In conclusion, the maximum of the trapping rate κ_{d2} obtained at $T_A = 650\,^{\circ}\mathrm{C}$ is probably caused by the increase in the microvoid density.

2. *p-type material*

The sample Si-*E* (*p*-type conductivity) was deformed in a similar way to samples Si-*B* and Si-*D*. The positron lifetime spectra were found to be completely different. Almost no positron trapping was observed, i.e., the average positron lifetime is close to the bulk level (as-deformed state: $\bar{\tau} = 226$ ps). Since the dislocation density is in the same range as Si-*B* and Si-*D*, we have to conclude that the sensitivity of the positrons for dislocations (defect d_1) is lost. Additionally, a similar number of microvoids is formed, since the same deformation procedure was applied as in Si-*B*. The positron trapping is also lost for this kind of defect d_2. A possible explanation is the electric field as a result of the local band-bending at the microvoid-bulk inner surface. It is expected to repel positrons in *p*-type material due to the repelling potential well.

B. Defect models

PA investigations of plastically deformed *p*-type silicon were published by Dannefaer *et al.* in 1983.[24] Si crystals were dynamically deformed at 800 °C up to or beyond the lower yield point and then isochronically annealed. Apparently, the samples were cooled without applied load, so that relaxation of the defect structure could occur. The authors found in the as-deformed state a defect lifetime of 420–480 ps, a value which steadily decreased by annealing at 750–900 °C down to 300 ps. The former lifetime was attributed to vacancy clusters and their thermal decay, the latter to PA at dislocations. Contrary to Dannefaer *et al.*,[24] neither remarkable positron trapping in *p*-type Si nor a continuous decrease of the positron trapping rates in *n*-type Si was observed in this study. The coexistence of positron trapping at microvoids and annihilation centers, which were dislocation related, could be monitored.

The most striking feature of HSLT-deformed crystals is the distinct increase of κ_{d2} without any remarkable change of τ_3 after 600 °C annealing in the samples Si-*B*, *C*, and *D*. If this feature is taken into consideration, the question of the vacancy supply mechanism arises. Since a formation of a microvoid with many vacancies by a single elementary step is extremely unlikely, a complex chain of clustering reactions with a competitive decay has to be considered, whereas only the final product is thermally stable at temperatures applied. Such a stable configuration may be an adamantine cage of ten vacancies V_{10} or a ringlike hexavacancy V_6, as they have been calculated by Chadi and Chang,[28] to be microvoids of minimum electronic total energy. Up to now, there has been no experimental verification of the presence of those structures.

However, the proposed hexavacancies V_6 do not form three-dimensional microvoids and thus, should not lead to such long positron lifetimes as observed. This is due to the only weak decrease of the electron density in a planar arrangement of vacancies.

The maximum of κ_{d2} at 600 °C annealing can be due either to agglomeration of vacancies already present (deformation induced) or to generation and clustering of vacancies by some dislocation relaxation mechanism. In the first case, the vacancies might be stabilized during deformation by the formation of vacancy-oxygen (*V-O*) pairs which form shallow positron traps with lifetimes close to the silicon bulk lifetime according to Mascher, Dannefaer, and Kerr.[29] Here, the following objection has to be made: According to Watkins, *V-O* pairs decay already at $T \approx 350$–$400\,^{\circ}\mathrm{C}$, which is considerably below the observed onset of thermal clustering.[30]

Therefore, vacancy generation and agglomeration during the thermal treatment itself, e.g., by dislocation relaxation, seems to be more likely. Recent TEM tilting experiments[31] show the existence of large jog densities (500 mm^{-1}) especially on edge dipoles after deformation at 800 °C used as the typical pretreatment before the HSLT step. The extension of these dislocations under HSLT conditions to hexagonal dislocation loops occurs in two steps: Especially in the early stage of HSLT deformation, jogs act as pinning points for dislocation motion, so short segments of 60° dislocations will be formed and extended. Depinning and dragging of jogs then leads in the course of the deformation to nonconservative motion of dislocations with screw components and therefore to vacancy emission and absorption on different tracks within the loops.

As an estimation typical values were used: $N_{\mathrm{dis}} = 5 \times 10^8\ \mathrm{cm}^{-2}$, the above-mentioned jog density of 500 mm^{-1} with a mean height of 20 lattice planes and dragging distances of 0.1 μm [which can be monitored by TEM (Ref. 32)]. This yields vacancy-interstitial concentrations of more than $10^{15}\ \mathrm{cm}^{-3}$. That way the occurrence of microvoids in deformed Si could be explained.

Supposing that EPR is able to identify the main defect groups formed during plastic deformation, the microvoids found by PA must be assigned to the subgroup Si-*K*3 to Si-*K*5.[4] These defects show the same annealing stage as the microvoids identified in this study. Furthermore, the density of the EPR centers was found to be in the same range in similarly deformed crystals.

The microvoids are dissolved by thermal treatment above 600 °C leading to an excess of vacancies. This fact may help to explain the experimental finding that dislocations in FZ silicon tend to climb by a decrease of the extra half plane during annealing at high temperature (i.e., motion by vacancy absorption; see Kisielowski-Kemmerich;[6] 800 °C annealing was used there). Regarding the crystals Si-*B* to *E*, it has to be assumed that additional jogs are formed by dislocation intersection processes during the extended glide at $T_{\mathrm{def}} = 390\,^{\circ}\mathrm{C}$. By line tensions those jogs are forced to move nonconservatively during the subsequent heat treatment and eventually annihilate as pairs. Both processes release vacancies or interstitials and give rise to the formation of additional mi-

crovoids at temperatures up to 600 °C. At this point, TEM investigations should be performed to elucidate the details of dislocation relaxation after long-time HSLT deformation and subsequent annealing in order to support the above hypotheses.

Regarding the long-lifetime component in germanium, results may be discussed in terms of similar underlying physical ideas of microvoid formation and stability by jog formation and motion, but it should be noted that the increase in κ_{d2} in the sample Ge-*B* at 350 °C coincides with the decrease in κ_{d1}. That may indicate a defect transformation: PA-active defects of divacancy character, presumably stabilized in or near the dislocation core, may be thermally released and clustered at the temperature mentioned above.

The results presented here corroborate the identification of the shorter lifetimes τ_2 with dislocation states. It should be noted that vacancy incorporation in the core of screw dislocations in silicon has been held responsible for the dislocation-related EPR centers $K1$, $K2$, and Si-Y.[6] It is likely that such defects within the dislocation core cause the dislocation-related PA. This would explain the annealing behavior of the trapping rate κ_{d1}.

But even perfectly reconstructed dislocations may attract positrons in their dilatation regions. The positron wave function can be smeared along the one-dimensional periodic potential of dislocations and the lifetime is increased versus the bulk value. However, a number of various dislocation types, which are likely differently sensitive to positrons, is formed during deformation. For instance, about 50% of the dislocations formed during the main deformation step are of the screw type. The share of screw dislocations is changed during annealing. It can be assumed at this stage of investigations that the screw dislocations (or their partials) are the PA-dominating part of the dislocations.

V. CONCLUSIONS

In positron lifetime studies of plastically deformed Si and Ge single crystals two positron lifetime components were separated. The shorter lifetime τ_2 (Si: 300 ps; Ge: 325 ps) was attributed to dislocations or dislocation-bound defects. The high third component τ_3 (Si: 590 ps; Ge: 520 ps) can only be ascribed to microvoids with effective radius $r \geq 0.4$ nm, corresponding to the number of vacancies involved $n \geq 10$.

The positron trapping to the microvoids was described as a diffusion-limited process. The trapping to dislocations was taken as diffusion limited as well, according to the measured temperature-dependent trapping rate. The densities obtained in this study for dislocations or microvoids agree satisfactorily with densities determined by TEM or EPR results previously obtained.

The maximum of the trapping rate of the microvoids after annealing at $0.5T_M$ is attributed to the increase of the microvoid density during annealing. The vacancy supply mechanism may be connected with dislocation climb. Supposing the model of depinning and dragging of jogs and using experimental values of the jog density and the dragging distance,[7,31] the required order of magnitude of the vacancy concentration for the formation of the microvoids can be obtained.

Two different capture models were discussed. It was concluded that the positron capture at microvoids and dislocations is independent of each other, but from PA results it cannot be conclusively excluded that the microvoids are bound to dislocations.

ACKNOWLEDGMENTS

The authors thank Professor A. Seeger and Dr. H. Gottschalk for fruitful discussions. The Deutsche Forschungsgemeinschaft is thanked for financial support.

[1]P. Omling, E. R. Weber, L. Montelius, H. Alexander, and J. Michel, Phys. Rev. B **32**, 6571 (1985).
[2]C. Kisielowski and E. R. Weber, Phys. Rev. B **44**, 1600 (1991).
[3]M. Stefaniak and H. Alexander, Appl. Phys. **A53**, 62 (1991).
[4]E. R. Weber and H. Alexander, Inst. Phys. Conf. Ser. **31**, 266 (1977).
[5]C. Kisielowski-Kemmerich and H. Alexander, in *Defects in Crystals,* edited by E. Mizera (World Scientific, Singapore, 1988), p. 290.
[6]C. Kisielowski-Kemmerich, Phys. Status Solidi B **161**, 11 (1990).
[7]M. Brohl, C. Kisielowski-Kemmerich, and H. Alexander, Appl. Phys. Lett. **50**, 1733 (1987).
[8]Y. H. Lee and J. W. Corbett, Phys. Rev. B **8**, 2810 (1973).
[9]G. Dlubek and R. Krause, Phys. Status Solidi A **102**, 443 (1987).
[10]S. Dannefaer, Phys. Status Solidi A **102**, 481 (1987).
[11]J. Mäkinen, C. Corbel, P. Hautojärvi, P. Moser, and F. Pierre, Phys. Rev. B **39**, 10 162 (1989).
[12]J. Mäkinen, P. Hautojärvi, and C. Corbel J. Phys. Condens. Matter **4**, 5137 (1992).
[13]M. J. Puska, C. Corbel, and R. M. Nieminen, Phys. Rev. B **41**, 9980 (1990).
[14]M. Brohl, M. Dressel, H. W. Helberg, and H. Alexander, Philos. Mag. B **61**, 97 (1990).
[15]A. Seeger, Appl. Phys. **4**, 183 (1974).
[16]W. Brandt, Appl. Phys. **5**, 1 (1974).
[17]L. Y. Xiong and C. W. Lung, in *Positron Annihilation,* edited by L. Dorikens-Vanpraet, M. Dorikens, and D. Seger (World Scientific, Singapore 1988), p. 374.
[18]A. Seeger, F. Banhart, and W. Bauer, in *Positron Annihilation,* edited by L. Dorikens-Vanpraet, M. Dorikens, and D. Segers (World Scientific, Singapore 1988), p. 275.
[19]M. Puska and C. Corbel, Phys. Rev. B **38**, 9874 (1988).
[20]S. Dannefaer, P. Mascher, and D. Kerr, J. Appl. Phys. **69**, 4080 (1991).
[21]K. Saarinen, C. Corbel, P. Hautojärvi, P. Lanki, F. Pierre, and D. Vignaud, J. Phys. Condens. Matter **2**, 2453 (1990).
[22]A. Seeger (private communication).
[23]W. Brandt and R. Paulin, Phys. Rev. B **5**, 2430 (1972).
[24]S. Dannefaer, N. Fruensgaard, S. Kupca, B. G. Hogg, and D. Kerr, Can. J. Phys. **61**, 451 (1983).
[25]W. Fuhs, U. Holzhauer, S. Mantl, F. W. Richter, and R. Sturm, Phys. Status Solidi B **89**, 69 (1978).

[26]E. Soininen, J. Mäkinen, D. Beyer, and P. Hautojärvi, Phys. Rev. B **46**, 13 104 (1992).
[27]A. Seeger and N. Banhart, Helv. Phys. Acta **63**, 403 (1990).
[28]D. J. Chadi and K. J. Chang, Phys. Rev. B **38**, 1523 (1988).
[29]P. Mascher, S. Dannefaer, and D. Kerr, Phys. Rev. B **40**, 11 764 (1989).
[30]G. D. Watkins, in *Deep Centers in Semiconductors,* edited by S. T. Pantelides (Gordon and Breach, New York 1986), p. 166.
[31]B. Ya. Farber and H. Gottschalk, in *Polycrystalline Semiconductors,* edited by J. H. Werner and H. P. Strunk (Springer-Verlag, Berlin 1991), p. 242.
[32]S. Sauerland, Diploma thesis, Universität Köln, 1990.

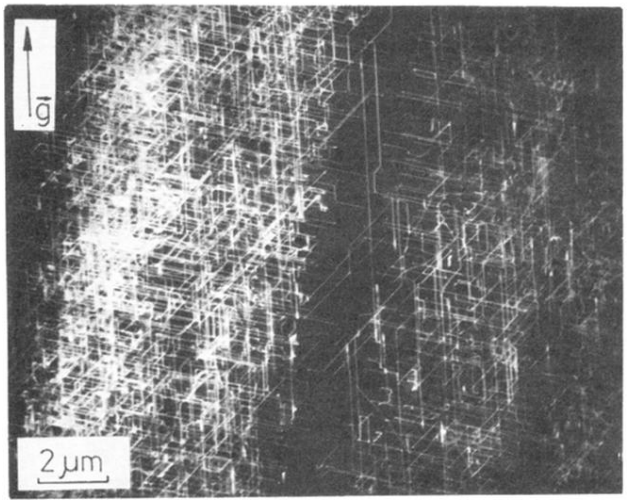

FIG. 9. Distribution of dislocations in Si-*C*. TEM weak beam (*g*-3*g* condition) taken at 1000 kV, (213) foil orientation, diffraction vector $\mathbf{g}=\bar{2}20$.